

doi:10.15199/48.2023.09.18

Pressure Regulation on A Single Finger of Tri-Finger Pneumatic Grasper Robot using Finite Time and Convergence Prescribed Performance Control.

Abstract. This study presents a method for improving the precision of pneumatic pressure regulation and control in a finger of a tri-finger pneumatic grasper (TPG) robot. The method employs finite time and convergence prescribed performance control (FTC-PPC) in conjunction with proportional, integral, and derivative (PID) control as a strategy to overcome the nonlinearity and uncertainties of pressure regulation of the pneumatic system in the TPG. Besides finite-time tuning, the proposed PPC formulation also introduced convergence rate and domain. To test the method, several experiments were conducted using a 5/3-way pneumatic proportional valve (PPV) configuration with pressure transducers for feedback responses. Two different pressure input patterns, a step, and periodic in-pulse patterns were used in the experiments. The results show that the proposed controller outperformed the PID as well as the finite-time PPC with PID from the previous works in regulating the pressure for a finger of the TPG by average. 10% in terms of minimizing overshoot, suppressing oscillations, and providing a fast response.

Streszczenie. W pracy przedstawiono metodę poprawy precyzji pneumatycznej regulacji i sterowania ciśnieniem w palcu trójpalcowego robota chwytaka pneumatycznego (TPG). Metoda wykorzystuje sterowanie wydajnością w określonym czasie i konwergencji (FTC-PPC) w połączeniu ze sterowaniem proporcjonalnym, całkującym i różniczkującym (PID) jako strategią przewyższenia nieliniowości i niepewności regulacji ciśnienia w układzie pneumatycznym w TPG. Oprócz dostrajania w skończonym czasie, proponowane sformułowanie PPC wprowadziło również szybkość i dziedzinę konwergencji. Aby przetestować tę metodę, przeprowadzono kilka eksperymentów przy użyciu konfiguracji pneumatycznego zaworu proporcjonalnego (PPV) 5/3 z przetwornikami ciśnienia do odpowiedzi sprzężenia zwrotnego. W eksperymentach wykorzystano dwa różne wzorce wejściowe ciśnienia, krok i okresowe wzorce wejściowe. Wyniki pokazują, że proponowany regulator przewyższał PID, a także skończony czas PPC z PID z poprzednich prac w regulacji ciśnienia na palec TPG średnio. (Regulacja ciśnienia na pojedynczym palcu trójpalcowego pneumatycznego robota chwytającego z wykorzystaniem skończonego czasu i zalecanej konwergencji kontroli wydajności)

Keywords: Pneumatic Robot System, Prescribed Performance Control, Pressure Control.

Słowa kluczowe: System robota pneumatycznego, zalecana kontrola wydajności, kontrola ciśnienia.

Introduction

The evolution of pneumatic systems in industrial automation has accelerated with the growth of computers, system integration, and information technology. This maturity has enhanced precision technology involving servoing, sensing, and control systems. In industrial automation, servopneumatics are becoming essential components primarily applied in providing precision machining and manufacturing processes [1-3]. In heavy-duty applications, such as compressed air energy storages, large-scale pneumatic robots, spacecrafts, and drilling machines, the use of high compressed energy-to-weight ratio force is common, because the system provides low-cost resources and low environmental emissions. From the robotics system perspective, pneumatic actuator or pneumatic servo system (PSS) is mainly applied and configured for soft robotic systems [4-7], designed with flexible mechanisms adaptable to the environment. In such systems, control system design must focus not only on displacement precision but also on dynamic motion. Therefore, pressure control and regulation play a crucial role because the strength of a pneumatic robot depends on the manipulation of air pressure. At this stage, controlling the valve system becomes a critical point because it affects the mass flow rate of gas, pressure regulation, and actuator motion direction.

Academicians, scholars, and engineers have made numerous approaches to improve this field, including various techniques, algorithms, and system integrations [8, 9]. For example, Gao et al. proposed a new aerostatic bearing system namely high-pressure electro-pneumatic servo valve (HESV) that directly driven by a voice coil motor (VCM) to improve the sensitivity of the spool motion as well as friction wear reduction. They also designed a hybrid fuzzy logic PID controller with disturbance observer to enhance and improve the performance of the proposed system[10]. In terms of intelligent valve positioner and stability, these systems are not only depending on the

advance of the hardware but also internal control algorithm. On the contrary, the control technique and algorithm design were emphasized in the study by Gahen *et. al* . The different perspectives on force and velocity control of pneumatic systems were proposed. Here the designed pulsating flow was generated to control the rod-piston of pneumatic system with solenoid coils for direction control on servo controllers[11]. On the other hand, the incremental nonlinear dynamic inversion (INDI) was introduced in the hybrid position and force control on the pneumatic system in a past study, which improved the robustness to the external disturbances without relying on plant information [12]. By involving an intelligent system, Liu *et. al* proposed a novel fuzzy cascade strategy on soft pneumatic system. The derived inverse Prandtl-Ishlinskii (P-I) model was used as the feed-forward component to cater the hysteresis and cascaded with the fuzzy-PID controller for pressure and position control [13]. However, the fuzzy indirect adaptive robust control algorithm (FIARC) was proposed in [14] to enhance error tracking control on pneumatic artificial muscle by employing a reconfigured radial basis function of fuzzy logic to compensate for parameter uncertainties of the model, control parameter deviation, and pneumatic muscle flow hysteresis aspects. A positive-negative pressure control was introduced in a past study to increase the precision of position and force control of pneumatic soft actuator with the disturbance observer to compensate for the coupled pressure dynamics of the negative and positive pressures [15]. Commonly, PID control is used wisely in industrial control system due to its simplicity and consistency. The difficulty in confronting nonlinear systems with substantial uncertainty such as pneumatic system has urged several efforts in enhancing the capability of this conventional control system [16-18]. However, the weakness remains, and the previous work on finite-time prescribed performance function (FT-PPF) in rod-piston precision shows a drawback in giving flexibility on

convergence time adjustment to cater further uncertainties such as oscillations in achieving fast transient [19, 20]. The previous works also emphasized on the precision and stability of the actuator part of the system, which did not emphasize thoroughly on the pressure with close tolerances to ensure the compressed air in pneumatic system is not wasted.

Therefore, this study focuses on providing soft-control on the pressure control and regulation of double acting cylinder (PPVDC) attached on a finger of TPG unit by using a novel finite-time with adjustable error convergence rate prescribed performance control (FTACR-PPC) to cater the error transformation suited to the hardware constraint and actual practice with PID as the inner-loop controller. The possibility of enhancing the Prescribed Performance Function (PPF) has made this function to be feasible for control system designers to practically implement and conjunct this system with other closed-loop control or inner-loop control system algorithm [21-23]. The paper is structured such that the overview of the TPG configuration as the experimental test rig is discussed in Section 2, the proposed finite-time prescribed performance control scheme with Proportional, Integral and Derivative (PID) is discussed in Section 3, the validation and analysis on the performance of proposed FTC-PPC with PID controller on a finger of TPG robot unit is discussed in Section 4, and the conclusion is drawn in Section 5.

Overview tri-finger pneumatic grasper system and configuration

The TPG was developed as a teaching and learning tool for the FANUC Robot S-430iF in the Faculty of Electrical and Electronics Engineering Technology at UMP, as illustrated in Fig. 1. The gripper is designed to handle large objects, such as cartons, boxes, and racks, in the industrial setting. It consists of three pneumatic pistons per finger and can perform two main functions: (1) gripping (GS) and (2) releasing (RS).

One of the fingers on the TPG is configured with a 5/3-way proportional valve (PPV), two pressure sensors (PS), and a rotary encoder at the joint, while the other two fingers have the standard ON/OFF solenoid valves without sensors. The PS are labeled as Port A (PA) and Port B (PB) with a default compressed air setting of 6 MPa (Fig. 2). Additionally, the pneumatic system utilizes an air compressor as the primary source of fluid power, which is configured with a pneumatic pressure regulator and filter to adjust the air pressure. Table 1 provides further details on the components and hardware system configuration setup of the TPG.

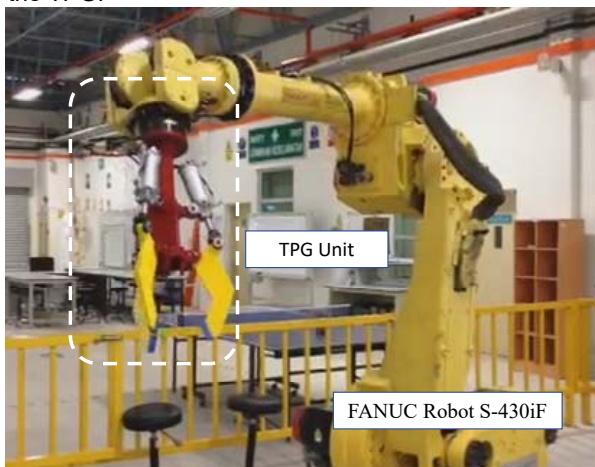


Fig. 1. Overview of TPG unit on Fanuc Robot.

Table 1. List of Components and Equipment for TPG unit

Equipment	Description
Proportional valve	Festo MPYE-5-1/4-010-B
Pressure regulator & filter	AirTAC SR200
Pressure transducer	Festo SPTW-P10R-G14-A-M12
Air compressor	SWAN SVP202 Air Compressor
Rotary encoder	500ppr
Fast switching pneumatic valve	Airtac 4v220-08 5 way 2 position 1/4" 12v

The TPG robot's flexibility is mainly derived from the finger configured with the 5/3-way PPV, which uses a multiple input and single output (MISO) control system structure. This structure is designed and set up with a real-time hardware-loop controller unit, using an STM32 microcontroller unit (MCU) as the main control unit, and programmed with MATLAB® SIMULINK software for real-time hardware-in-loop implementation.

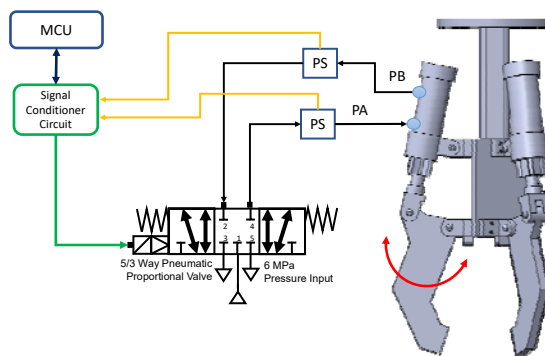


Fig. 2. Overview of pneumatic system setup for a finger of TPG unit with proportional closed-loop control

Controller design

The strategy of pressure control and regulation for a single finger of TPG robot with PPV system is configured by focusing on PA because both ports have a similar flow in operation. The pressure is controlled and regulated from the error tracking of the pressures between pressure reference input (P_d) and pressure feedback response at PA (P_A) that can be computed at finite-time (t) as follows:

$$(1) \quad e(t) = P_d(t) - P_A(t)$$

In previous works as reported [19, 20], FT-PPC shows its ability to encountered the finite-time conditions as compared to conventional PPC in providing tunable converge according to the system constraints. Tunable converge rate is crucial in prescribing the transient period of the error states in tracking control. Therefore, the study has proposed a new FT-PPF with the new exponential that can be computed using the expression as follows:

$$(2) \quad \rho(t) = (\rho_0 - \rho_\infty) \Lambda + \rho_\infty$$

where,

$$(3) \quad \Lambda = e^{-\frac{\beta(t)^2}{t_0^2}}$$

with

$$(4) \quad \beta(t) = \lambda_1 t \left(\tanh \left[\lambda_2 (t - t_0) \right] + 1 \right)$$

where λ_1 and λ_2 are the positive finite value for scaling factor with default value of 1 for both finite time and converge rate for Eq. 2. Additionally, another component that has been enable for adjustment with certain constraint

is a domain of the decay function $(\bar{\sigma}, \underline{\sigma})$. This adjustment method allowing $\bar{\sigma} \neq \underline{\sigma}$ whereby the domain can be determined as Eq.5:

$$(5) \quad \begin{aligned} \bar{\sigma}_A &= (\bar{\sigma} - 1)\Lambda + 1 \\ \underline{\sigma}_A &= (\underline{\sigma} - 1)\Lambda + 1 \end{aligned}$$

where adjustable domain $(\bar{\sigma}_A, \underline{\sigma}_A)$ with the constraint as shown in Eq. 6.

$$(6) \quad \begin{aligned} \lim_{t \rightarrow \infty} \bar{\sigma}_A &> 1, \quad \bar{\sigma} \geq 1 \\ \lim_{t \rightarrow \infty} \underline{\sigma}_A &> 1, \quad \underline{\sigma} \geq 1 \end{aligned}$$

Then, the boundary of performance function can be justified with the range as in Eq. 7:

$$(7) \quad -\underline{\sigma}_A \rho(t) < e(t) < \bar{\sigma}_A \rho(t), \forall t > 0$$

where $e(t)$ represents tracking error as depicted in Eq. 1. As for the next step of the design, an error transformation is presented to convert the origin constrained tracking error, $e(t)$, to unconstrained tracking error. The transformation is to demonstrate the relationship between $\rho(t)$ and $e(t)$. The equation to compute the transformation of $e(t)$ is as follows:

$$(8) \quad e(t) = \rho(t)S(\varepsilon)$$

where ε is developed to the increase the function $S(\varepsilon)$ and can be obtained because the function of $|e(t)| < \rho(t), \forall t \geq 0$ is strictly increasing monotonously. Conversely, defining $\rho(t)$ can enable the control of both transient response and steady error input of the closed-loop controller. The inverse transformation function for the bounded $\varepsilon(t)$ can be computed as follows:

$$(9) \quad \varepsilon(t) = S^{-1}\left(\frac{e(t)}{\rho(t)}\right) = \frac{1}{2} \ln\left(\frac{\psi(t)+1}{1-\psi(t)}\right)$$

where $\varepsilon(t)$ is the new transformed tracking error variable, $S^{-1}(\bullet)$ is the inverse function of $S(\varepsilon)$ and normalized error $\psi(t) = e(t)/\rho(t)$ at $|\varepsilon(0)| < 1$. Furthermore, $\psi(t)$ satisfies $-1 < \psi(t) < 1$ whenever $\varepsilon(t) \neq \infty$ and the predefined bound of PPF [24] is guaranteed whenever $\varepsilon(t)$ is constantly bounded. The boundary is determined by Eq. 8 with the pre-defined $\rho(t)$. Thus, control input (u) of integration between FTACR-PPC with PID controller can be expressed as follows:

$$(10) \quad u(t) = K_p \varepsilon(t) + K_i \int \varepsilon(t) dt + K_d \frac{d}{dt} \varepsilon(t)$$

where $\{K_p, K_i, K_d\} > 0$ are the continuous positive finite design parameters. Fig.3 depicts the overall control system architecture for PPVDC pressure control and regulation using the proposed FTC-PPC with PID controller.

Results and discussion

Experimental tests were conducted to validate the control performances of the proposed FTC-PPC with PID controller (FTCP-PID) on a finger of TPG robot as shown in

Fig. 4. The tests were divided into two sessions with different patterns of pressure input: step and periodical pressure inputs. The parameters for FTCP-PID were fine-tuned periodically according to the FTC-PPC framework's transformation error compliances. According to the current platform, the period between 0 and 1 s is considered as an idle period whereby FTC-PPC will be triggered after 1 s of operation. The final value of PID and FTC-PPC parameters after fine-tuned are tabulated in Table 2. The comparison study was done by comparing the FPPC-PID with the PID controller alone as well as the FT-PPC with PID (FT-PID) that was used for rod-piston position on the same platform in pervious works [20].

Table 2. Fine-tuned values of tuning parameters for FTC-PPC and PID

Controller	Parameters	Values
PID	K_p	65
	K_i	0.55
	K_d	0.81
FTC-PPC	λ	9
	ρ_0	3MPa
	ρ_∞	0.5MPa
	$\bar{\sigma}$	1
	$\underline{\sigma}$	1
	t_0	0.3
	λ_1	1
λ_2	3	

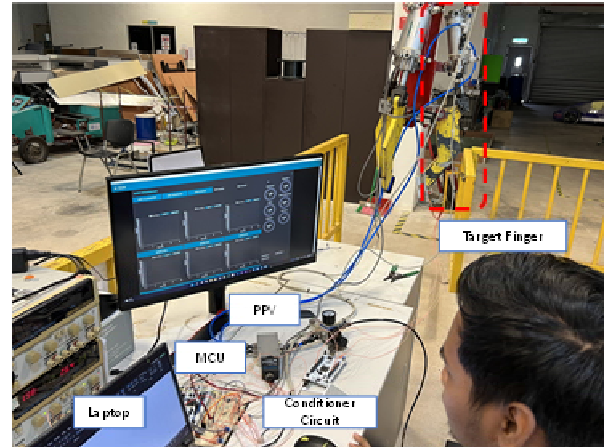


Fig. 4. Experiment Setup

The first experiment was attempted using a step input trajectory to test the pressure regulation, which is a basic test for PSS to verify the response to fast changes in inputs. The step input pressures that needed to be regulated were set in a range between 0 and 4 MPa. Fig. 5 shows that the FTCP-PID was very stable and precise in the pressure regulation from the first positioning, compared to the PID as well as the FT-PID in the overall view of displacement results with the step trajectory. The pressure regulation using FTCP-PID was able to reduce the transient period by about 10% compared to the regulation process that only used FT-PID and far better than the regulation that used PID only at about 70%. The improvement by the FTCP-PID was noticeable early on, after the transient state of the step pressure reference. The proposed FTCP-PID was able to increase the settling time by 10%, considerably faster than the FT-PID controller and the PID.

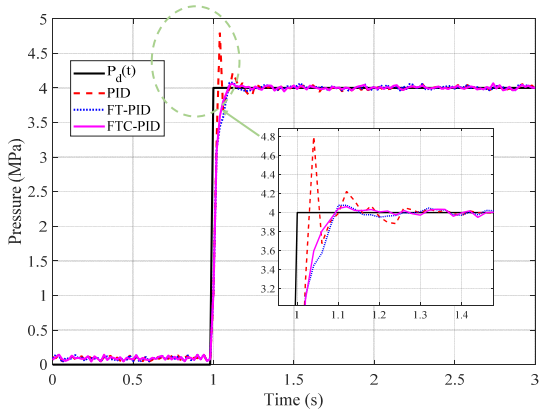


Fig. 5. Sample of pressure regulation with step input

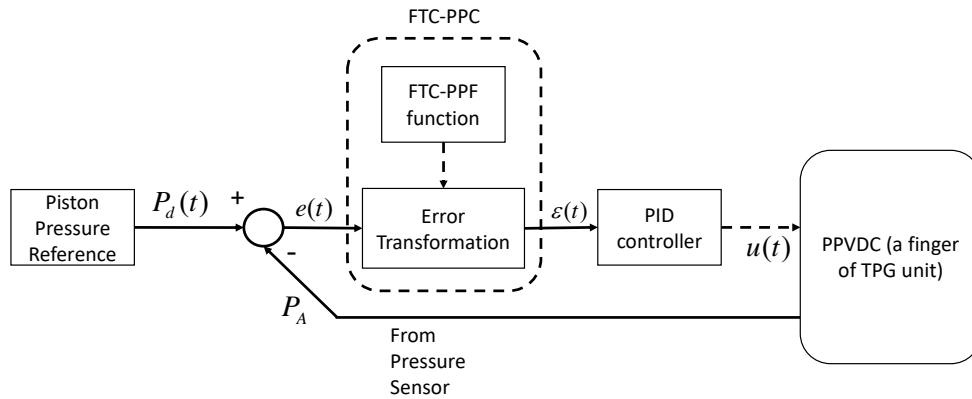


Fig. 3. Overall Control System Structure of Pressure Control using PID with proposed FTC-PPC on a Single Finger of TPG with PPVDC unit.

The brief duration and amplitude of the pressure chamber spike indicate a reduced possibility of overshoot and oscillation in the rod-piston's motion, leading to significant reductions in tracking errors. The effect of this approach is apparent in the performance of the FTCP-PID controller (Fig. 7), where the controllable air pressure in both pneumatic cylinder chambers facilitated smooth piston positioning, and tracking errors were considerably reduced compared to the FT-PID and PID controllers (Fig. 5). A summary of the controller's overall performance for the PPVDC system is provided in Table 3.

or phase shift between the desired input and feedback response [25] by applying a periodic pressure input on the targeted PPVDC to actuate the robot's finger. The periodic pressure input reference was a 0.25-Hz sine wave with a peak-to-peak amplitude ranging from 1.5 to 4.5 MPa.

Table 3. Summary of performance for each controller with step pressure input

Performance	Controller		
	PID	FT-PID	FTCP-PID
Steady-state error	0.01MPa	0.003MPa	0.00001MPa
Rise time	0.005ms	0.0012	~0.0001ms
Settling time	3s	3s	2.7s
Percentage of max overshoot	10.4 %	1.85%	0.08 %

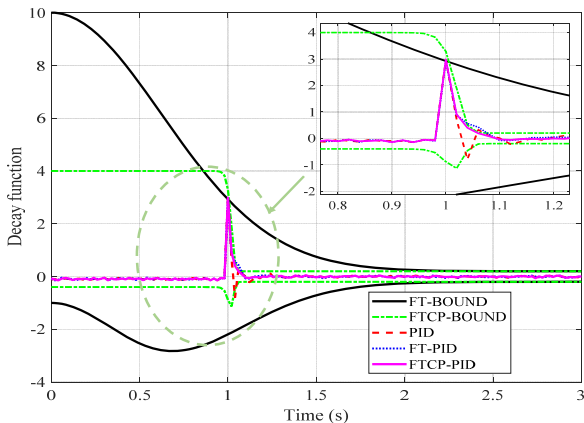


Fig. 6. Sample of tracking error performance in PPF convergence time boundaries

The experiment was further continued with the periodical pressure input test. The test was conducted to evaluate the proposed controller's ability to reduce the constant time lag

The test was divided into two sections with different initial inputs: (1) zero and (2) nonzero. Both sections used the same fine-tuned gain setup listed in Table 2. Fig. 8 shows that the FTCP-PID controller effectively handled oscillation and minimized overshoot when the input signal suddenly stepped from zero to a certain value at the beginning of the operation. Compared to the FT-PID and PID controllers, the FTCP-PID controller exhibits an outstanding response to the desired pressure input pattern. Fig. 8 also indicates that neglecting the hardware system acquisition sampling time of 1 ms resulted in a steady-state error of about ± 0.0125 MPa mean square average from the desired input for pressure regulation using the FTCP-PID controller. This error is approximately 36% lower than that of the FT-PID controller in terms of steady-state or tracking error performance. The results also demonstrate that the

FTCP-PID controller could suppress high oscillation behavior by nearly 80% compared to the PID controller.

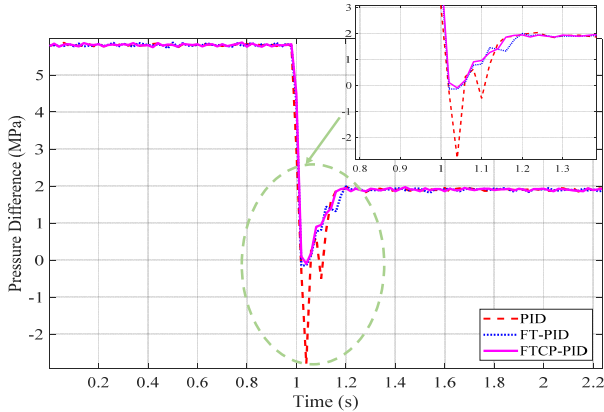


Fig. 7. Sample of different pressures in cylinder

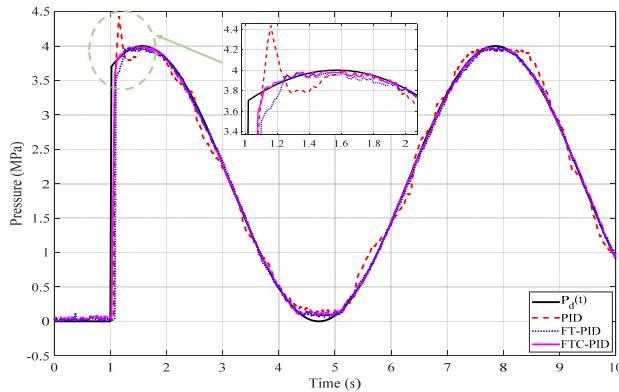


Fig. 8. Sample of pressure regulation with sinusoidal input at zero initial point

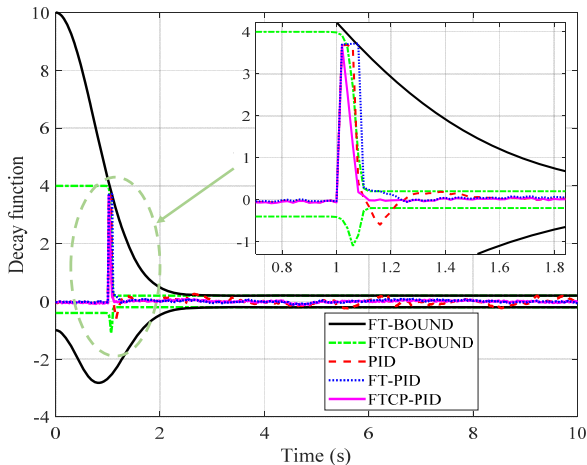


Fig. 9. Sample of tracking error performance in PPF convergence time boundaries at zero initial point

Fig. 9 shows the tracking errors for FTCP-PID were smaller and the convergence rate was earlier than that of the FT-PID at about 1 s. The early small domain shown by the FTCP-PID also indicates that the steady-state error was more stable in terms of oscillation reduction compared to the FT-PID and PID. A slightly different phenomenon occurs when the pressure input reference has a nonzero initialization. Fig. 10 shows that the pressure regulation with FT-PID failed to attain a steady state in a short period compared to the FTCP-PID. This suggests that the controller had a delay in response because it delayed about

1.5 s compared to the FTCP-PID controller. On the other hand, the PID controller performed even worse, where a very high delay occurred in the pressure response of about 5.5 s later than both FTCP-PID and FT-PID controllers. This poor performance is further evident in the PPF performances in Fig. 11, where the pressure steady-state error with FTCP-PID is always in-bounded compared to the FT-PID. Similar to the test with a zero initial point, the fast convergence rate and small domain of FTCP-PID enable it to reduce the overshoot in transient response and suppress oscillation earlier than the FT-PID from 1 to 1.4 s As shown in Fig. 11.

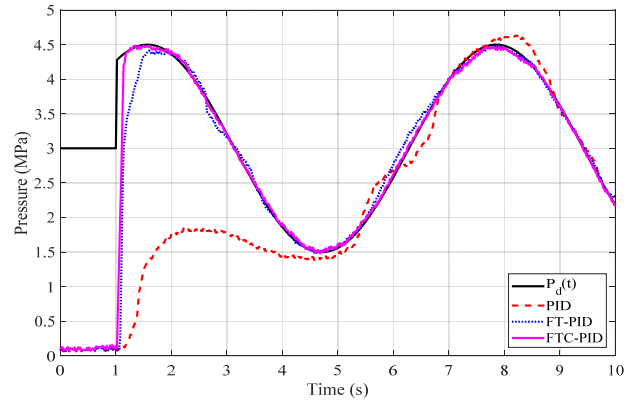


Fig. 10. Sample of pressure regulation with sinusoidal input at nonzero initial point

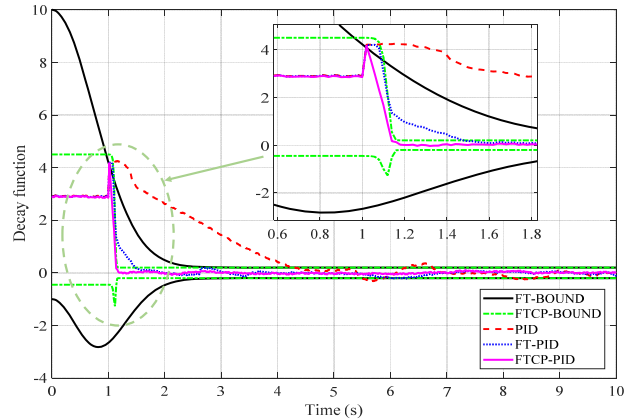


Fig.11. Sample of tracking error performance in PPF convergence time boundaries at non-zero initial point

Conclusion

This study presented and validated the pressure regulation and control using the proposed FTC-PPC with PID controller to PPS as an actuator for the finger of the TPG robot. The proposed controller demonstrates superiority in several aspects, including stable and precise pressure regulation and control. The most significant findings indicate that the proposed method with FTC-PPF provides stable transient and fast response, in addition to improving the overall tracking error performances. The constant time lag between the desired input and feedback response can also be minimized with the proposed FTC-PPC in periodical input tests. The overall results demonstrate that this method is practical and applicable for any fluid actuated system, such as the TPG robot, particularly designed for heavy-duty tasks in industrial applications. An optimization study on PPF parameter determination and tuning would be an interesting topic for future research.

ACKNOWLEDGEMENT

The authors would like to thank the Universiti Malaysia Pahang under the Postgraduate Research Grant (PGRS2003158) for providing financial support as well as laboratory facilities. Also, thank to Ministry of Higher Education Malaysia for providing financial support under Fundamental Research Grant Scheme (FRGS) No. FRGS/1/2019/TK04/UMP/02/1 (University reference RDU1901106).

Authors: Assoc. Prof. Dr. Addie Irawan, Robotics, Intelligent & Control Engineering (RISC) Research Group, Faculty of Electrical & Electronics Engineering Technology, Universiti Malaysia Pahang, 26600, Pekan, Pahang, Malaysia, E-mail: addieirawan@ump.edu.my [Corresponding]

Mohd Iskandar Putra Azahar, Robotics, Intelligent & Control Engineering (RISC) Research Group, Faculty of Electrical & Electronics Engineering Technology, Universiti Malaysia Pahang, 26600, Pekan, Pahang, Malaysia, E-mail: iskandarputra1995@gmail.com

Dr. Mohd Syakirin Ramli, Intelligent & Control Engineering (RISC) Research Group, Faculty of Electrical & Electronics Engineering Technology, Universiti Malaysia Pahang, 26600, Pekan, Pahang, Malaysia, E-mail: syakirin@ump.edu.my.

REFERENCES

- [1] M. L. Dezaki, S. Hatami, A. Zolfagharian, and M. Bodaghi, "A pneumatic conveyor robot for color detection and sorting," *Cognitive Robotics*, vol. 2, pp. 60-72, 2022/01/01/ 2022, doi: <https://doi.org/10.1016/j.cogr.2022.03.001>.
- [2] J. Dong, J. Shi, C. Liu, and T. Yu, "Research of Pneumatic Polishing Force Control System Based on High Speed On/off with PWM Controlling," *Robotics and Computer-Integrated Manufacturing*, vol. 70, p. 102133, 2021/08/01/ 2021, doi: <https://doi.org/10.1016/j.rcim.2021.102133>.
- [3] H. Chang, C.-w. Lan, C. H. Chen, T.-T. Tsung, and J.-B. Guo, "Measurement of frictional force characteristics of pneumatic cylinders under dry and lubricated conditions," *Przegląd Elektrotechniczny*, 2012.
- [4] R. Gkliva and M. Kruusmaa, "Soft Fluidic Actuator for Locomotion in Multi-Phase Environments," *IEEE Robotics and Automation Letters*, vol. 7, no. 4, pp. 10462-10469, 2022, doi: [10.1109/LRA.2022.3192204](https://doi.org/10.1109/LRA.2022.3192204).
- [5] L. Costi, J. Hughes, J. Biggins, and F. Iida, "Bioinspired Soft Bendable Peristaltic Pump Exploiting Ballooning for High Volume Throughput," *IEEE Transactions on Medical Robotics and Bionics*, vol. 4, no. 3, pp. 570-577, 2022, doi: [10.1109/TMRB.2022.3192763](https://doi.org/10.1109/TMRB.2022.3192763).
- [6] L. P. Johnsen and H. Tsukagoshi, "Deformation-Driven Closed-Chain Soft Mobile Robot Aimed for Rolling and Climbing Locomotion," *IEEE Robotics and Automation Letters*, vol. 7, no. 4, pp. 10264-10271, 2022, doi: [10.1109/LRA.2022.3191798](https://doi.org/10.1109/LRA.2022.3191798).
- [7] M. I. P. Azahar, A. Irawan, and R. M. Taufika, "Fuzzy Self-Adaptive PID for Pneumatic Piston Rod Motion Control," in *ICSGRC 2019 - 2019 IEEE 10th Control and System Graduate Research Colloquium, Proceeding*, 2019, pp. 82-87, doi: [10.1109/ICSGRC.2019.8837064](https://doi.org/10.1109/ICSGRC.2019.8837064).
- [8] A. N. Frederik Stefanski, Bartosz Minorowicz, "Pneumatic single flappper nozzle valve driven by piezoelectric tube," *Przegląd Elektrotechniczny*, vol. 2015, no. 1, pp. 13-19, 2015.
- [9] K. K. Jarosław Domin, "Hybrid pneumatic-electromagnetic launcher - general concept, mathematical model and results of simulation," *Przegląd Elektrotechniczny*, vol. 12, pp. 21-25, 2013.
- [10] L. Gao, C. Wu, D. Zhang, X. Fu, and B. Li, "Research on a high-accuracy and high-pressure pneumatic servo valve with aerostatic bearing for precision control systems," *Precision Engineering*, vol. 60, pp. 355-367, 2019/11/01/ 2019, doi: <https://doi.org/10.1016/j.precisioneng.2019.09.005>.
- [11] O. A. Gaheen, E. Benini, M. A. Khalifa, and M. A. Aziz, "Pneumatic cylinder speed and force control using controlled pulsating flow," *Engineering Science and Technology, an International Journal*, p. 101213, 2022/07/25/ 2022, doi: <https://doi.org/10.1016/j.jestch.2022.101213>.
- [12] H. Das, D. Pool, and E. J. v. Kampen, "Incremental Nonlinear Dynamic Inversion Control of Long-Stroke Pneumatic Actuators," in *2021 European Control Conference (ECC)*, 29 June-2 July 2021 2021, pp. 978-983, doi: [10.23919/ECC54610.2021.9654927](https://doi.org/10.23919/ECC54610.2021.9654927).
- [13] Z. Liu, X. Yin, K. Peng, X. Wang, and Q. Chen, "Soft pneumatic actuators adapted in multiple environments: A novel fuzzy cascade strategy for the dynamics control with hysteresis compensation," *Mechatronics*, vol. 84, p. 102797, 2022/06/01/ 2022, doi: <https://doi.org/10.1016/j.mechatronics.2022.102797>.
- [14] S. Dan, H. Cheng, Y. Zhang, and H. Liu, "A Fuzzy Indirect Adaptive Robust Control for Upper Extremity Exoskeleton Driven by Pneumatic Artificial Muscle," in *2022 IEEE International Conference on Mechatronics and Automation (ICMA)*, 7-10 Aug. 2022 2022, pp. 839-846, doi: [10.1109/ICMA54519.2022.9856383](https://doi.org/10.1109/ICMA54519.2022.9856383).
- [15] C. Park et al., "Simultaneous Positive and Negative Pressure Control Using Disturbance Observer Compensating Coupled Disturbance Dynamics," *IEEE Robotics and Automation Letters*, vol. 7, no. 2, pp. 5763-5770, 2022, doi: [10.1109/LRA.2022.3160599](https://doi.org/10.1109/LRA.2022.3160599).
- [16] A. Tepljakov, B. B. Alagoz, C. Yeroglu, E. Gonzalez, S. H. HosseinNia, and E. Petlenkov, "FOPID Controllers and Their Industrial Applications: A Survey of Recent Results11This study is based upon works from COST Action CA15225, a network supported by COST (European Cooperation in Science and Technology)," *IFAC-PapersOnLine*, vol. 51, no. 4, pp. 25-30, 2018/01/01/ 2018, doi: <https://doi.org/10.1016/j.ifacol.2018.06.014>.
- [17] M. Muftah and A. Faudzi, "Fractional-Order PI λ D μ Controller for Position Control of Intelligent Pneumatic Actuator (IPA) System," 2021, pp. 242-250.
- [18] M. I. P. Azahar, A. Irawan, and R. M. T. Raja Ismail, "Adjustable Convergence Rate Prescribed Performance with Fractional-Order PID Controller for Servo Pneumatic Actuated Robot Positioning," *Cognitive Robotics*, Article vol. 3, pp. 93-106, 2023, doi: [10.1016/j.cogr.2023.04.004](https://doi.org/10.1016/j.cogr.2023.04.004).
- [19] M. I. P. Azahar, A. Irawan, and M. S. Ramli, "Transient Control Improvement on Pneumatic Servoing in Robot System using Fractional-Order PID with Finite-time Prescribed Performance Control," in *2022 IEEE 12th Symposium on Computer Applications & Industrial Electronics (ISCAIE)*, 21-22 May 2022 2022, pp. 206-210, doi: [10.1109/ISCAIE54458.2022.9794510](https://doi.org/10.1109/ISCAIE54458.2022.9794510).
- [20] M. I. P. Azahar and A. Irawan, "Enhancing Precision on Pneumatic Actuator Positioning using Cascaded Finite-time Prescribed Performance Control," in *2021 11th IEEE International Conference on Control System, Computing and Engineering (ICCSCE)*, Penang, Malaysia, 27-28 Aug. 2021 2021, pp. 131-136, doi: [10.1109/ICCSCE52189.2021.9530956](https://doi.org/10.1109/ICCSCE52189.2021.9530956).
- [21] S. Gao, X. Liu, Y. Jing, and G. M. Dimirovski, "A novel finite-time prescribed performance control scheme for spacecraft attitude tracking," *Aerospace Science and Technology*, vol. 118, p. 107044, 2021/11/01/ 2021, doi: <https://doi.org/10.1016/j.ast.2021.107044>.
- [22] J. Lin, H. Liu, and X. Tian, "Neural network-based prescribed performance adaptive finite-time formation control of multiple underactuated surface vessels with collision avoidance," *Journal of the Franklin Institute*, vol. 359, no. 11, pp. 5174-5205, 2022/07/01/ 2022, doi: <https://doi.org/10.1016/j.jfranklin.2022.05.048>.
- [23] S. Luo, X. Wu, C. Wei, Y. Zhang, and Z. Yang, "Adaptive finite-time prescribed performance attitude tracking control for reusable launch vehicle during reentry phase: An event-triggered case," *Advances in Space Research*, vol. 69, no. 10, pp. 3814-3827, 2022/05/15/ 2022, doi: <https://doi.org/10.1016/j.asr.2022.02.049>.
- [24] M. I. P. Azahar, A. Irawan, and M. S. Ramli, "Finite-Time Prescribed Performance Control for Dynamic Positioning of Pneumatic Servo System," in *2020 IEEE 8th Conference on Systems, Process and Control (ICSPC)*, Melaka, Malaysia, 11-12 Dec. 2020 2020, pp. 1-6, doi: [10.1109/ICSPC50992.2020.9305755](https://doi.org/10.1109/ICSPC50992.2020.9305755).
- [25] M. I. P. Azahar, A. Irawan, and R. M. T. R. Ismail, "Self-tuning hybrid fuzzy sliding surface control for pneumatic servo system positioning," *Control Engineering Practice*, vol. 113, p. 104838, 2021/08/01/ 2021, doi: <https://doi.org/10.1016/j.conengprac.2021.104838>.